ISSN 0021-8944, Journal of Applied Mechanics and Technical Physics, 2018, Vol. 59, No. 5, pp. 912–921. © Pleiades Publishing, Ltd., 2018.
Original Russian Text © V.A. Ivanov, T.Ya. Shul'ga.

IMPACT OF ATMOSPHERIC FRONT PARAMETERS ON FREE AND FORCED OSCILLATIONS OF LEVEL AND CURRENT IN THE SEA OF AZOV

V. A. Ivanov and T. Ya. Shul'ga

UDC 551.465.75 (262.54)

Abstract: Level and current oscillations in the basin of the Sea of Azov have been studied by hydrodynamic modeling using the Princeton ocean model (POM). The hypothesis on the role of the resonance mechanism in the occurrence of extremely large amplitudes of storm surge and seiche oscillations depending on the velocity and time of motion of atmospheric fronts of the Sea of Azov has been tested. It is found that at the same wind, pressure perturbations moving over the Sea of Azov induce forced oscillations, and after the perturbations cease, free oscillations with amplitudes that are 14% higher than those obtained at constant atmospheric pressure. It is shown that the motion of the atmospheric front (whose velocity and time are selected under the assumption that waves with maximum amplitudes are generated) plays an important but not decisive role in the formation of the structure of currents and level oscillations in the Sea of Azov.

Keywords: Sea of Azov, sigma-coordinate model, free oscillations of liquid, seiches, stationary currents, storm surges, nodal lines, atmospheric front, free long wave velocity.

DOI: 10.1134/S002189441805019X

INTRODUCTION

Level and current oscillations in the seas and are induced by various external and internal forces, whose influence leads to different-scale oceanic processes with periods of a few seconds to several decades. Of great importance in the development of extreme levels and hydrological processes in the coastal areas of the Sea of Azov are storm surges, seiche, and seiche-like waves with periods of several hours to several days [1]. In this processes, the structure of dominant longitudinal natural oscillations is such that their peaks are located near large settlements [2, 3]. Therefore, it is of interest to study the influence of seiche-like waves on the development of level oscillations with extreme amplitudes and currents of the Sea of Azov.

A major factor responsible for seiche-like oscillations in natural water basins is a change in atmospheric pressure. Sharp pressure changes in different parts of a water reservoir set the entire mass of the reservoir water in oscillatory motion. Seiches with a significant amplitude arise when a resonance occurs, i.e., when the period of natural oscillations in the basin coincides with the period of the acting force. Furthermore, the relatively low pressure gradient at the boundaries of the reservoir and their corresponding small level differences cause significant seiches. The pressure front moving over the water surface with a velocity close to the free long wave velocity induces extreme storm surges, which, after the cessation of atmospheric perturbations, are transformed into seiches with a large amplitude.

The behavior of waves in the region of atmospheric fronts has been studied for a relatively short time, and there is no sufficient experience in predicting free and forced oscillations under the indicated conditions [4–6].

Marine Hydrophysical Institute, Russian Academy of Sciences, Sevastopol 299011, Russia; vaivanov@inbox.ru; shulgaty@mail.ru. Translated from Prikladnaya Mekhanika i Tekhnicheskaya Fizika, Vol. 59, No. 5, pp. 166–177, September–October, 2018. Original article submitted October 13, 2017; revision submitted January 9, 2018.

The dynamics of natural marine basins under the influence of mesoscale atmospheric processes is of scientific and practical interest. Investigation of seiche-like oscillations in the Sea of Azov and an analysis of field observation data were carried out in [2]. In [3], seiche oscillations of level and current occurring in the Sea of Azov as a result of 1-m storm surges at the open boundary were studied using a linear two-dimensional mathematical model.

The present work is a continuation of the studies [7, 8] of free and forced level oscillations in the Sea of Azov using the three-dimensional hydrodynamic Princeton ocean model (POM) [9]. The development of currents, storm surges and seiche-like oscillations in the Sea of Azov in the atmospheric pressure perturbation field has been studied based on an analysis of the results of numerical simulation. The hypothesis on the role of the resonance mechanism in the occurrence of extremely large amplitudes of storm surges and seiche oscillations generated by a pressure front moving over the sea with a velocity equal to the velocity of free long waves [10]. In this case, the period of perturbing pressures is equal to the period of natural oscillations of the liquid in the basin. Space-time features of seiche-like oscillations arising after passage of atmospheric formations have been established. Dependences of the characteristics of storm surges and seiches on atmospheric parameters are inferred.

FORMULATION OF THE PROBLEM. MODEL AND ITS PARAMETERS

Mathematical modeling of free and forced oscillations in the Sea of Azov was conducted using the POM three-dimensional barotropic nonlinear sigma-coordinate model [9] based on a system of differential equations describing sea dynamics. Due to the shallowness of the Sea of Azov, which has a significant effect on the hydrological situation in the water basin, the thermal and dynamic inertia of the waters of this sea is small. This makes it possible to use simpler barotropic hydrodynamic models [11] which take into account the variable depth of the reservoir, the Coriolis force, the variable atmospheric pressure, and the friction at the bottom and the free surface:

$$\frac{du}{dt} - fv + \frac{1}{\rho}\frac{\partial P}{\partial x} = 2\frac{\partial}{\partial x}\Big(A_M\frac{\partial u}{\partial x}\Big) + \frac{\partial}{\partial y}\Big[A_M\Big(\frac{\partial v}{\partial x} + \frac{\partial u}{\partial y}\Big)\Big] + \frac{\partial}{\partial z}\Big(K_M\frac{\partial u}{\partial z}\Big); \tag{1}$$

$$\frac{dv}{dt} + fu + \frac{1}{\rho}\frac{\partial P}{\partial y} = 2\frac{\partial}{\partial y}\Big(A_M\frac{\partial v}{\partial y}\Big) + \frac{\partial}{\partial x}\Big[A_M\Big(\frac{\partial v}{\partial x} + \frac{\partial u}{\partial y}\Big)\Big] + \frac{\partial}{\partial z}\Big(K_M\frac{\partial v}{\partial z}\Big); \tag{2}$$

$$\frac{\partial P}{\partial z} + g\rho = 0; \tag{3}$$

$$\frac{\partial u}{\partial x} + \frac{\partial v}{\partial y} + \frac{\partial w}{\partial z} = 0. \tag{4}$$

Here x, y, and z are spatial variables (the x axis is directed to the east, the y axis is directed to the north, and the z axis is directed vertically up), t is time, $u(x, y, z, t)$ and $v(x, y, z, t)$ are the horizontal flow velocity components, $w(x, y, z, t)$ is the vertical flow velocity component, $P(x, y, z, t) = P_{\text{atm}} + g\rho_0(\zeta - z)$ is the pressure at depth z obtained by integration of (3); $P_{\text{atm}} = 1013.25$ hPa is the standard atmospheric pressure at a temperature of 0°C at a latitude of 45°, ρ is the density of water, $\rho_0 = \dfrac{1}{\zeta + H}\displaystyle\int_{-H}^{\zeta}\rho\, dz$ is the depth-mean water density, g is the acceleration of gravity, f is the Coriolis parameter, K_M is the vertical turbulent viscosity coefficient determined using the Mellor–Yamada theory [12]; A_M is the horizontal turbulent viscosity coefficient calculated by the Smagorinsky formula [13].

On the sea surface, we specify the universal condition for the vertical components w and the boundary conditions for the horizontal velocity component in the form of a momentum flux which depends on the friction stresses caused by the wind:

$$w\Big|_{z=\zeta} = \frac{\partial\zeta}{\partial t} + u\frac{\partial\zeta}{\partial x} + v\frac{\partial\zeta}{\partial y}, \qquad K_M\Big(\frac{\partial u}{\partial z}, \frac{\partial v}{\partial z}\Big)\Big|_{z=\zeta} = (\tau_{0x}, \tau_{0y}), \tag{5}$$

where $(\tau_{0x}, \tau_{0y}) = \rho_a c_a |\boldsymbol{U}_W| (u_W, v_W)$ [14], $\boldsymbol{U}_W$ is the wind velocity at a standard height of 10 m above the sea water surface, u_W and v_W are the wind velocity components, ρ_a [kg/m^3] is the air density under standard atmospheric conditions, and c_a is the surface friction coefficient which depends on the wind velocity.

At the bottom, we impose no-flow conditions expressed by the kinematic boundary condition indicating the absence of flow normal to the boundary and by the quadratic parametrization of the bottom friction:

$$\Big(w + u\,\frac{\partial H}{\partial x} + v\,\frac{\partial H}{\partial y}\Big)\Big|_{z=-H} = 0, \qquad K_M\Big(\frac{\partial u}{\partial z}, \frac{\partial v}{\partial z}\Big)\Big|_{z=-H} = (\tau_{1x}, \tau_{1y}), \tag{6}$$

where $(\tau_{1x}, \tau_{1y}) = c_b|\boldsymbol{U}_b|(u_b, v_b)$, u_b and v_b are the horizontal flow velocity components at grid points near the bottom of the basin, c_b is the bottom friction coefficient which is chosen to be the maximum of the values calculated using the logarithmic law and a value of the empirical constant equal to 0.0025: $c_b = \max\{k^2(\ln(H + z_b)/z_0)^{-2}; 0.0025\}$ ($z_0 = 3$ cm is the roughness parameter, z_b is the grid node closest to the bottom, and $k = 0.4$ is the von Kármán constant).

For the velocity at the lateral boundaries, we specify the conditions of the absence of normal flow $\boldsymbol{U_n} = 0$ and no-slip $\boldsymbol{U_\tau} = 0$, where $\boldsymbol{n}$ and $\boldsymbol{\tau}$ are the normal and tangential directions, respectively. The initial (for $t = 0$) conditions are taken to be the absence of liquid motion and the condition that the free surface is horizontal before the onset of atmospheric perturbations.

The model was discretized on a C-grid, and the transfer operators were approximated using the TVD-scheme. In the original equations (1)–(4), boundary conditions (5), (6), and the initial conditions, the transition from the coordinate z to the coordinate σ [9] is performed. Uniform steps along the horizontal coordinates $\Delta x = \Delta y = 1.4$ km and along the σ-coordinate are used. The steps of integration along the time and space coordinates are chosen in accordance with the stability criterion for barotropic waves [15]. The depth values for describing the bottom relief in the computational domain are taken from navigation charts.

Observations in marine water areas crossing or contacting the continents have shown that in transitional seasons, frontal regions occur which move with a velocity of 30–35 km/h (8–10 m/s) and can travel a distance of 600–800 km in a day. The width of the front surface is several dozens of kilometers and covers the water area of the Sea of Azov. The wind modes and water surface oscillations ahead of and behind the front are significantly different. At the fronts, especially cold ones, there are significant gradients of air temperature, humidity, and other meteorological parameters that can cause a sharp increase of wind to a squall one [16].

Scenarios of the passage of seasonal atmospheric fronts over the Sea of Azov were reproduced in computational experiments (Fig. 1). The boundaries between the pressure regions move along one of the given trajectories: meridional (see Fig. 1a), zonal (see Figs. 1b and 1d), and diagonal (see Fig. 1c). The values of the pressure gradient, the width of the front region, and their values in the regions of high and low pressures were adopted based on an analysis of generalized reference hydrometeorological data [16].

The velocity and time of motion of the pressure field are chosen under the assumption waves with maximum amplitudes are generated. This is possible when the period of the driving force approaches the period of natural oscillations in the basin. In this case, the pressure front moving above the water surface with a velocity close to the value of $\sqrt{gH}$ causes high surges near the coast, resulting in large-amplitude seiches [10].

The time t_f of motion of the front over the entire sea area is set equal to the time of the greatest rise in the level of the Sea of Azov, which occurs during the half-period of the highest mode of free oscillations. Its value is determined from observation data and results of analytical calculations. Thus, in [2, 3], seiches with periods $T_{\text{observ}} = 6$–7 and $T_{\text{observ}} = 23$ h were observed. Theoretical values of the periods T_{Merian} were obtained by the Merian formula with the Rayleigh correction [2]:

$$T_{\text{Merian}} = \frac{2L}{\sqrt{gh}}\,(1 + \varepsilon), \qquad \varepsilon = \frac{b}{\pi l}\Big(\frac{3}{2} - \ln\frac{\pi b}{l} - C_\varepsilon\Big), \tag{7}$$

where $C_\varepsilon = 0.5772$ is the Euler constant, $L = 360$ km is the length of the sea (along the Genichesk–Pereboinyi line), $h = 10$ m is the average depth of the sea, $b = 30.6$ km is the width of the strait at the entrance to Taganrog Bay, and $l = 137$ km is the length of Taganrog Bay. The period of the first mode calculated by formula (7) is equal to 24.1 h.

Thus, comparing the values of T_{observ} and T_{Merian}, we assume that the dominant longitudinal natural oscillations of the first mode of the Sea of Azov level have a period approximately equal to $T \approx 24$ h. The structure of this mode is such that one of its vertices is located in Taganrog Bay and the opposite vertex is near Genichesk. Therefore, it is of interest to study the influence of inhomogeneous pressure fields on the occurrence of storm surges and seiche-like oscillations in these areas.

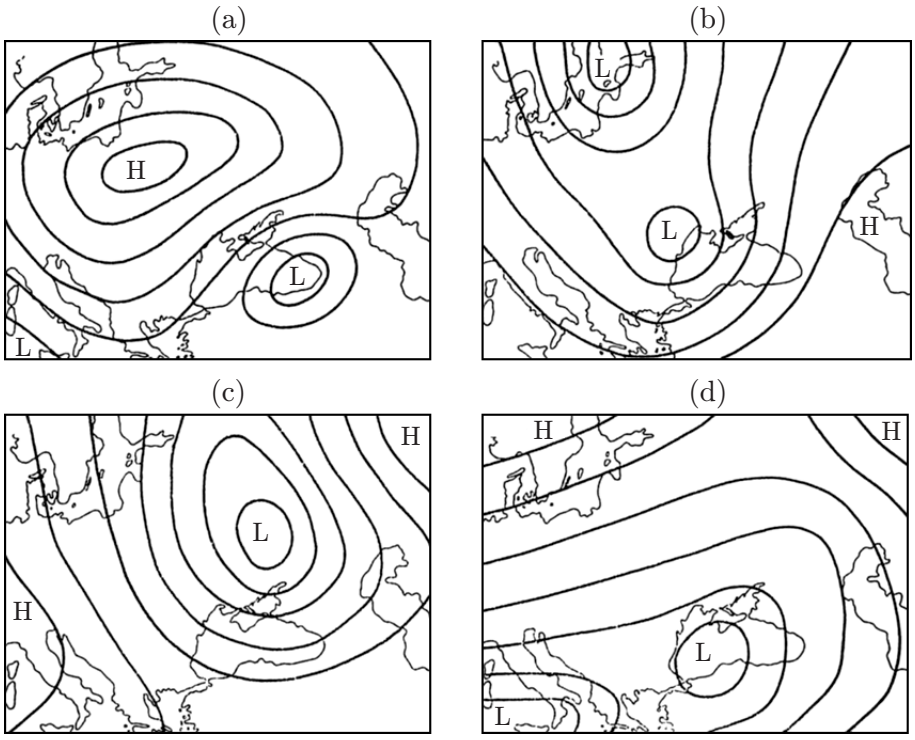

Fig. 1. Pressure fields during the passage of seasonal atmospheric fronts over the Sea of Azov: (a) anticyclone formed over the central regions of European Russia; (b) anticyclone formed over Asia Minor and Kazakhstan; (c) anticyclone with a wedge above the Balkan Peninsula; (d) Mediterranean cyclones; H and L denote high- and low-pressure regions.

To test the hypothesis of the occurrence of extreme seiches due to a change in atmospheric pressure in different parts of the sea, we performed two series of numerical experiments. The conditions of the experiments differed in the resonant mechanisms of formation of maximum-amplitude storm surges and seiche oscillations in the Sea of Azov. In the first series of experiments, a characteristic of the pressure front is the period of action of the inhomogeneous atmospheric pressure field, which is a multiple of the period of natural oscillations of the basin, and in the second series of experiments, it is the velocity close to the free long wave velocity.

In each experiment, the development of the front occurs in the field of background stationary flows, and the beginning of the motion of the front corresponds to the time of the establishment of liquid motion ($t_{\rm st} = 48$ h) [7]. Stationary motions in the Sea of Azov are generated by southwestern wind uniform in time and space with velocity $|\boldsymbol{U}_W| = 10$ m/s. At this stage ($0 \leqslant t \leqslant t_{\rm st}$), the atmospheric pressure is constant throughout the water area of the sea and its value is equal to the standard atmospheric pressure $P_{\rm atm}$.

The next stage of the experiment corresponds to the passage of a non-uniform field of atmospheric pressure over the water area the Sea of Azov. At the moment of the beginning of its motion ($t_{\rm st} = 48$ h), the sea water area is divided into the region D over which the pressure is constant and equal to the normal atmospheric pressure $P_{\rm atm}$ and the region $\bar{D}$ over which an inhomogeneous pressure field moves. The dimensions of the regions D and $\bar{D}$ change with time and are limited by the dimensions of the computation grid of the Sea of Azov basin ($0 \leqslant x \leqslant x_{\max} = 350$ km, $0 \leqslant y \leqslant y_{\max} = 250$ km). The function $P_a(x, y, t)$ which simulates the pressure in the atmospheric front is given by two different analytical expressions for the regions D and $\bar{D}$:

$$P_a(x, y, t) = P_{\rm atm} = \text{const}, \quad (x, y) \in D, \qquad P_a(x, y, t) = P_{\rm atm} + a(t - t_{\rm st}), \quad (x, y) \in \bar{D}, \tag{8}$$

and also depends on the time, which varies in the range $t_{\rm st} \leqslant t \leqslant t_f$. The coefficient a is chosen in such a way that the function $P_a(x, y, t)$ has a unique jump with an amplitude equal to the pressure gradient along the front line near the surface $[a(t_f - t_{\rm st}) = \Delta P_{\rm fr}]$. In this case, $\Delta P_{\rm fr}$ is calculated from the wind velocity value known in this experiment using the formula $|\boldsymbol{U}_W| = 0.7\sqrt{(4.8/\sin\varphi)^2(\Delta P_{\rm fr}^2 + \alpha^2 \Delta t_{\rm fr}^2) + 64}$ proposed in [17] ($\Delta t_{\rm fr}$ is the air temperature difference in the front zone at a distance of 50 km, α is the transition coefficient, and φ is the latitude).

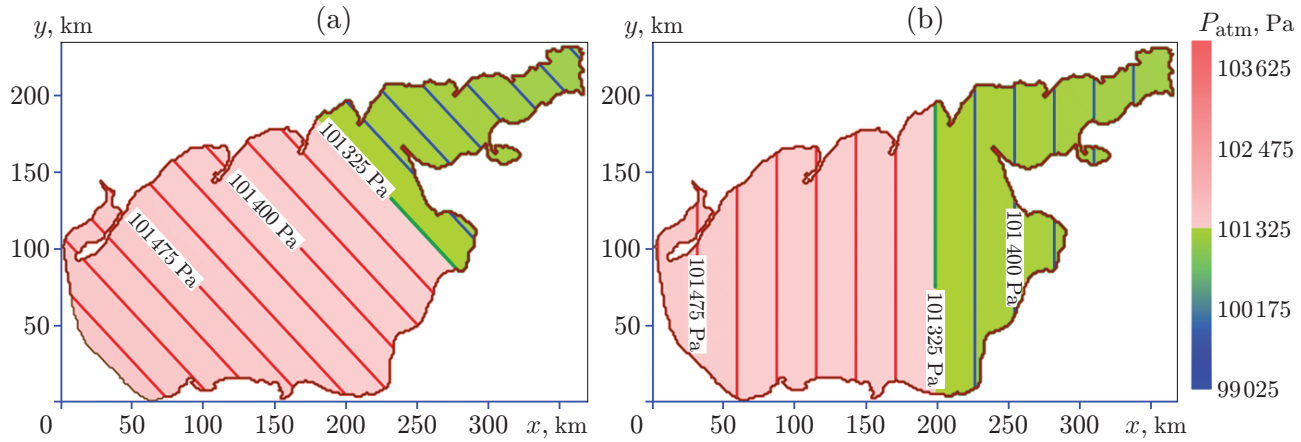

Fig. 2. Trajectories of motion of the fronts of variable atmospheric pressure with a velocity of 8 m/s in the Genichesk–Pereboinyi direction for different slopes of the boundaries to the x axis: 135° (a) and 90° (b).

The regions of constant and variable atmospheric pressure (D and $\bar{D}$) are located on both sides of the front line γ, whose position depends on the current coordinates x and y and time t. The spatial curve γ is defined parametrically: $x = x(t)$ and $y = y(t)$. The type of parametric equations determines the configuration of the front lines: the straight lines with a certain slope and curves with a given curvature radius. The velocity and time of motion of the perturbing pressure fields in the water area of the Sea of Azov are determined from the velocity $\boldsymbol{U}_\gamma$ and the time of motion of the front edge t_f. For the indicated series of numerical experiments, these values are obtained in different ways.

For the first series of numerical experiments, the period of atmospheric perturbations t_f is chosen to be a multiple of the period (T) of the highest mode of free oscillations of the Sea of Azov. In this case, the modulus of the velocity of the front boundary is found from the formula $|\boldsymbol{U}_\gamma| = 2L/T$. For the second series of calculations, the velocity of the atmospheric pressure boundary is a variable quantity equal to the free long wave velocity which depends on the depth of the sea ($|\boldsymbol{U}_\gamma(H)| = \sqrt{gH}$). In this case, the time of action of atmospheric perturbations at different velocities of their motion is different and is also determined from the relation $t_f = L/|\boldsymbol{U}_\gamma(H)|$.

ANALYSIS OF THE RESULTS

The mathematical model was used to calculate the magnitude of extreme storm surges caused by pressure perturbations,and the maximum characteristics of free oscillations in the Sea of Azov after passage of atmospheric fronts. The magnitudes of the level amplitudes, flow velocities, and periods of seiche-like oscillations are analyzed on the basis of data obtained at coastal stations and in the central parts of the basin.

Taganrog Bay, located in the northeastern part of the Sea of Azov, is an almost rectangular basin with a length of 137 km and a maximum width of 30 km. The single-node longitudinal seiche dominating in Taganrog Bay influences the formation of storm surges, and this influence can be significant when the periods of natural and forced oscillations coincide.

The purpose of the numerical experiments is to study the effect of the pressure front on the free and forced oscillations in the Sea of Azov level, whose time of passage is equal to the period of natural oscillations in the basin. Air moves from the high-pressure region to the low-pressure region under the influence of a pressure gradient. At the moment the air is set in motion, the Coriolis force begins to act and deflect the air flow to the right. With an increase in wind velocity, the flow deflection also increases under the action of the Coriolis force, resulting in the geostrophic wind moving along the isobar rather than from the high-pressure region to the low-pressure region.

The trajectories of motion of inhomogeneous pressure fronts over the Sea of Azov adopted in the numerical experiments are shown in Fig. 2. The pressure field isolines correspond to the time 9 h, which is counted from the moment the low-pressure regions begin to move. Figure 2 shows the propagation of these regions with a velocity $|\boldsymbol{U}_\gamma| = 8$ m/s in the Genichesk–Pereboinyi direction. These regions differ in the geometry of the boundary γ: in Fig. 2a, this is a straight line with a slope to the x axis equal to 135 °, and in Fig. 2b, the boundaries between pressure regions move along a diagonal trajectory (with a slope to the x axis equal to 90°).

Table 1. Values of Stationary Storm Surges ($\zeta_{\rm st}$) under the Action of a Stationary Wind with a velocity of 10 m/s and the Extrema of the Amplitudes of the Forced ($\zeta_{\rm extr}$) and the First Two Seiche-Like Oscillations ($\zeta_{1,2}$) at the Corresponding Times $t_{1,2}$ at Constant Atmospheric Pressure and after the Passage of the Pressure Front with a Velocity of 8 m/s

Station	$P_{\rm atm}$					$P_a(x,y,t)$				
	$\zeta_{\rm st}$, m	ζ_1, m	t_1, h	ζ_2, m	t_2, $\zeta_{\rm extr}$, m	ζ_1, m	t_1, h	ζ_2, m	t_2, h	
Genichesk	2.02	−0.27	9.5	0.33	16.5	2.15	−0.28	10.0	0.39	16.8
Berdyansk	0.25	−0.57	2.5	0.46	7.7	0.25	−0.60	2.8	0.48	7.7
Mariupol	−1.53	−0.01	12.3	−0.20	20.2	−1.82	−0.01	12.5	−0.21	20.6
Taganrog	−1.58	−0.89	24.3	0.30	31.5	−1.64	−0.97	24.4	0.35	31.5
Eisk	−2.44	−0.06	18.3	0.21	28.5	−2.62	−0.07	18.7	0.25	28.9
Primorsko-Akhtarsk	−1.75	0.92	5.3	−0.10	13.9	−1.88	0.95	5.5	−0.10	13.9
Temryuk	−0.18	1.03	2.7	−0.14	13.5	−0.18	1.07	3.1	−0.14	13.6
Opasnoe	0.32	0.93	1.7	−0.08	13.0	0.37	0.93	2.2	−0.09	13.1
Mysovoe	0.98	−0.20	8.7	0.26	15.4	1.06	−0.22	8.7	0.30	15.6

The calculated extreme deviations of sea level obtained at constant pressure and during the passage of an inhomogeneous pressure front under the action of the same stationary western wind with a velocity of 10 m/s are given in Table 1. The table gives the maximum and minimum values of sea-level deviations at coastal stations of the Sea of Azov at the time of wind cessation ($\zeta_{\rm st}, \zeta_{\rm extr}$) and the first successive extrema of the amplitudes of seiche oscillations $\zeta_{1,2}$ at their corresponding times $t_{1,2}$ counted from the moment $t_{\rm st}$ at constant pressure $P_{\rm atm}$ and for passage with a velocity of 8 m/s through the entire water area at the variable pressure $P_a(x,y,t)$ calculated by formula (8).

From Table 1 it follows that the wind causes maximum stationary up-surges at the Genichesk station (2.02 m) and down-surges at the Eisk (2.44 m), Primorsko-Akhtarsk (1.75 m), and Taganrog (1.58 m) stations. Comparison with the extrema of the amplitudes of the level deviations caused by the passage of the pressure front shows that the greatest differences at the indicated stations are 14%.

Using the data in Table 1, we analyze the seiche-like oscillations recorded at the stations where the largest storm surges take place. At the Eisk station, where the greatest down-surge occurs [−2.44 m ($t = t_{\rm st}$)], the cessation of the wind causes a rise in sea level [$\zeta_1 = -0.06$ m ($t_1 = 18.3$ h)]. In this case, the amplitude of the first oscillation is 2.38 m. Then the level continues to rise, and in 10.2 h, it reaches the maximum value of 0.21 m; the amplitude of the second oscillation (0.27 m) is 8.8 times smaller than the amplitude of the first oscillation.

The passage of the pressure front leads to a change in the amplitude and periods of free oscillations, which at the Eisk station are significantly different. Thus, at the moment of cessation of perturbations, due to the lowering of the level by 2.62 m, free oscillations with amplitudes of 2.55 and 0.32 m are generated. Note that the magnitude of the stationary down-surge at this station is 7% smaller than that of the nonstationary one, the difference in the amplitudes of seiche oscillations does not exceed 16%, and their periods are 0.5 h. Since, in both cases, waves and currents are generated by a wind of the same strength, this difference is obviously due to the passage of the pressure front with a pressure gradient of 100 GPa.

Figure 3 shows the fields of the current velocity modulus w in the surface water layer of the Sea of Azov obtained for steady-state motion at the moment of wind cessation and at regular intervals (3 h) from the moment of the cessation of all external influences. It can be seen that for different wind velocities, the current velocity maxima are shifted toward Taganrog Bay. Zero current velocities are observed at different points of the water area. In this case, currents of opposite directions correspond to the same direction of motion of the pressure perturbation boundary over the water area.

In the second series of experiments, we analyzed the influence of resonance characteristics which depend on the free long wave velocity. The velocity of atmospheric pressure fields $|\boldsymbol{U}_\gamma(H)| = \sqrt{gH}$ over the water area is calculated using the dispersion relation and depends on the depth of the basin.

Table 2 shows the dependence of the extreme amplitudes of level oscillation in the Sea of Azov on the velocity of the pressure perturbation boundary in the meridional direction in the field of a constant west wind with a velocity of 10 m/s. The velocity of the pressure front, similar to the free long wave velocity, changes for different selected sea depths (7–14 m).

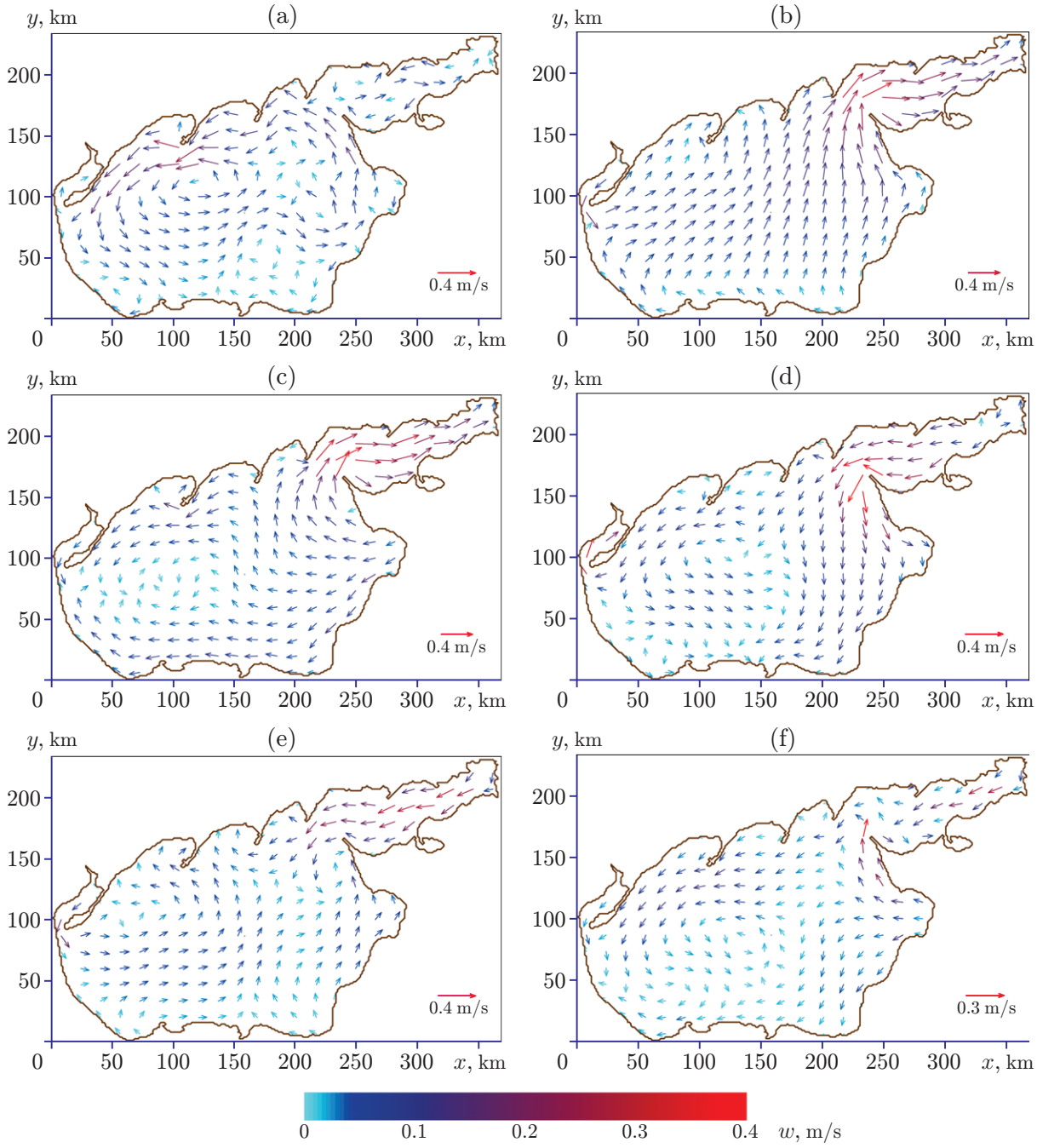

Fig. 3. Fields of the flow velocity modulus w in the Sea of Azov for steady-state motion (a), at the time of wind cessation (b), and at different times after the wind cessation: in 3 h (c), 6 h (d), 9 h (e), and 12 h (f).

Comparison of the data presented in Table 2 with the results of calculations performed for a constant atmospheric pressure [7] confirms the hypothesis of the influence of moving baric formations on the level and current oscillations in the Sea of Azov. Thus, during the passage of pressure fronts, the extreme amplitudes of level oscillations and maximum current velocities ($\zeta_{\max} = 0.56$ m, $\zeta_{\min} = 0.4$ m, and $|\boldsymbol{U}|_{\max} = 0.26$ m/s) increase by 20, 23, and 14%, respectively, compared to the case of constant atmospheric pressure P_{atm}.

Table 2. Extreme Characteristics of Currents versus Velocity of Atmospheric Pressure Fronts $|\boldsymbol{U}_\gamma(H)|$ over the Sea of Azov

$\lvert\boldsymbol{U}_\gamma(H)\rvert$, m/s	$\zeta_{\max}$, m	$\zeta_{\min}$, m	$\lvert\boldsymbol{U}\rvert_{\max}$, m/s
8,3	0.56	0.40	0.26
8.9	0.66	0.46	0.27
9.4	0.74	0.52	0.30
9.9	0.70	0.50	0.28
10.4	0.68	0.48	0.24
10.9	0.64	0.44	0.23
11.3	0.58	0.40	0.22
11.7	0.58	0.40	0.21

It follows from Table 2 that the velocity of motion of pressure perturbations affects the maximum velocities and deviations of sea level. The greatest values of these quantities are attained at a velocity of the front $|\boldsymbol{U}_\gamma(H)| = 9.4$ m/s, which corresponds to a sea depth of 9 m. The time of passage of this baric formation from the westernmost to the easternmost boundary of the Sea of Azov is 10 h 40 min. Note that the front moving for a longer time, e.g., with a velocity of 8.3 m/s (12.8 h) has a less significant effect on the parameters of wave motions.

Using the results of the experiment, we investigate the change in the free-surface level at the moment the liquid motion becomes steady-state and during the passage of the atmospheric perturbation over the sea water area at regular intervals (3 h) from the moment of cessation of all external influences.

Figure 4 shows the results of numerical simulation of the motion a pressure perturbation over the Sea of Azov from west to east in the field of a constant wind blowing with a velocity of 10 m/s in the same direction. In this case, the interface between the air masses with an atmospheric pressure gradient moves with a velocity equal to the free long wave velocity ($|\boldsymbol{U}_\gamma(H)| = 8.29$ m/s) calculated for a mean sea depth of 7 m. The time of passage of the atmospheric front is chosen equal to half the period of free oscillations ($t_f = T_{\text{Merian}}/2 = 12$ h).

In the case of steady-state motion (see Fig. 4a), the water dynamics is determined by the nodal line passing through the center of the basin and the maximum amplitudes in the western and eastern parts of the basin. With the development of the free oscillation process, the generation of vortex perturbations enhances and the nodal line asymmetrically rotates counterclockwise, being located along the x axis(see Fig. 4b) and diagonally to it (see Fig. 4c). In 3 h after the wind cessation (see Fig. 4c), the free oscillations are a two-node seiche with the central nodal line similar to its configuration in the initial period of time [$t = t_{\text{st}}$ (see Fig. 4a)]. The two shorter nodal lines are symmetric and have the shape of semicircles whose diameters are perpendicular to the direction of the atmospheric front.

The lowest intensity of free level oscillations is observed in the central region of the basin. In 6 h after the wind cessation (see Fig. 4d), the system of two-node seiches moves eastward, with the greatest deviations in the level occurring in the opposite corners of the basin. With the further development of the free oscillations (see Figs. 4e and 4f), the small nodal lines are combined into a single line passing along the diagonal of the basin and dividing it into regions of increasing and decreasing level.

CONCLUSIONS

Based on the results of the numerical simulation, it is established that perturbations moving with a velocity close to the free long wave velocity leads to generation of waves with larger amplitudes than those generated at the same wind and constant atmospheric pressure. The greatest amplitudes of level oscillations are caused by the motion of pressure fields with a velocity of 9.4 m/s. The passage of pressure fields along the Genichesk–Pereboinyi line for a time equal to half the period of natural oscillations of the basin gives rise to forced oscillations and then to free oscillations with amplitudes differing by not more than 14% from those obtained at constant atmospheric pressure and the same wind.

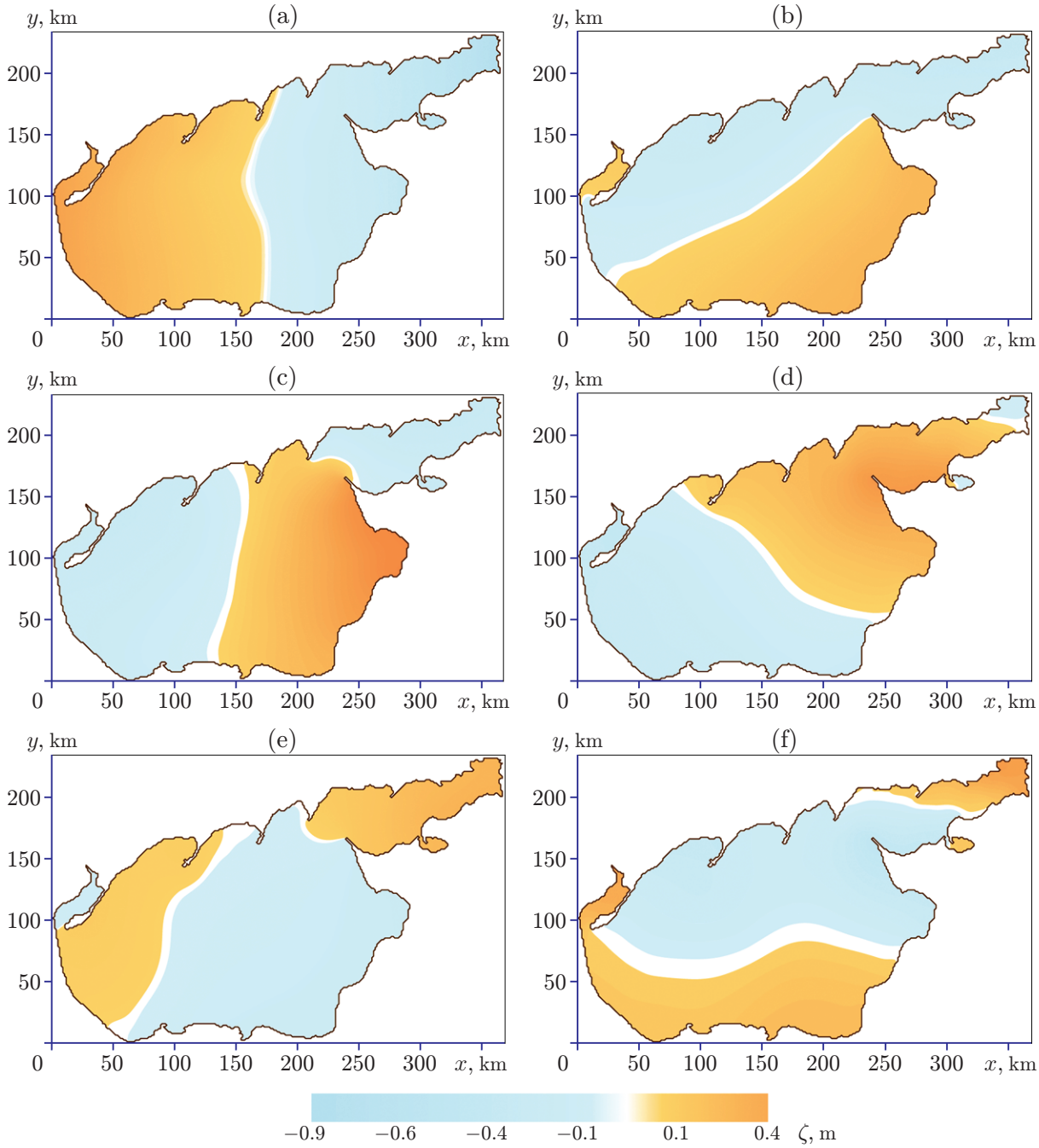

Fig. 4. Level isolines in the Sea of Azov at the same times as in Fig. 3.

Atmospheric pressure perturbation influences the structure of currents and level oscillations in the Sea of Azov level. The same direction of motion of the pressure perturbation boundary over the sea water can correspond to opposite-direction currents which depend only on the direction of the wind. The processes caused by long-term constant winds have a significant effect on currents and levels.

This work was carried out within the framework of State Task No. 0827-2014-0010 “Complex Interdisciplinary Studies of Oceanological Processes That Determine the Functioning and Evolution of the Black Sea and the Sea of Azov Ecosystems Based on Modern Methods of Monitoring the State of the Marine Environment and Grid Technologies.”

REFERENCES

1. A. S. Monin, "Classification of Nonstationary Processes in the Ocean," Izv. Akad. Nauk SSSR, No. 7, 26–30 (1972).
2. V. Kh. German, "Investigation and Calculation of the Probabilistic Characteristics of Extreme Sea Levels," Tr. Gos. Okeanograf. Inst., No. 107, 1971.
3. G. G. Matishov and Yu. I. Inzhebeikin, "Numerical Studies of Seiche-Like Level Oscillations in the Sea of Azov," Okeanologiya **49** (4), 485–493 (2009).
4. K. M. Sirotov and T. M. Sidel'nikova, "Experience in Calculating the Wind Velocity and Wave Height in the Cold Front Zone," Tr. Gidromettsentra SSSR, No. 263, 72–75 (1984).
5. F. L. Bykov and V. A. Gordin, "Objective Analysis of the Structure of Atmospheric Fronts," Izv. Ross. Akad. Nauk, Fiz. Atmos. Okeana **48** (2), 172–188 (2014).
6. A. L. Chikin, "Two-Layer Mathematical Model of Wind Currents in Water Reservoirs Having Large Shallow Regions," Mat. Model. **21** (12), 152–160 (2009).
7. V. A. Ivanov, L. V. Cherkesov, and T. Ya. Shu'lga, "Dynamic Processes and Their Influence on the Transformation of Passive Impurities in the Sea of Azov," Okeanologiya **54** (4), 464–472 (2014).
8. V. A. Ivanov, L. V. Cherkesov, and T. Ya. Shul'ga, "Free Oscillations of the Sea of Azov Level Arising after the Cessation of a Long-Term Wind," Mor. Gidrofiz. Zh., No. 2, 15–24 (2015).
9. A. F. Blumberg and G. L. Mellor, "A Description of the Three-Dimensional Coastal Ocean Circulation Model," in *Three-Dimensional Coastal Ocean Models* (Amer. Geophys. Union, Washington, 1987), Vol. 4, pp. 1–16.
10. N. A. Labzovskii, *Non-Periodic Sea Level Oscillations* (Gidrometeoizdat, St. Petersburg, 1971) [in Russian].
11. V. S. Vasil'ev and A. I. Sukhinov, "Precision Two-Dimensional Models of Shallow Water Bodies," Mat. Model. **15** (10), 17–34 (2003).
12. G. L. Mellor and T. Yamada, "Development of a Turbulence Closure Model for Geophysical Fluid Problems," Rev. Geophys. Space Phys. **20**, 851–875 (1982).
13. J. Smagorinsky, "General Circulation Experiments with Primitive Equations. 1. The Basic Experiment," Monthly Weather Rev. **91** (3), 99–164 (1963).
14. W. Wannawong, Usa W. Humphries, P. Wongwises, and S. Vongvisessomjai, "Mathematical Modeling of Storm Surge in Three-Dimensional Primitive Equations," Int. Comp. Math. Sci. **5** (6), 497–806 (2011).
15. R. Courant, K. O. Friedrichs, and H. Lewy, "On the Partial Difference Equations of Mathematical Physics," IBM J. Res. Develop. **11** (2), 215–234 (1967).
16. *Hydrometeorological Conditions of the Shelf Zone of the Seas of the USSR*, Vol. 3: *Sea of Azov* (Gidrometeoizdat, Leningrad, 1986) [in Russian].
17. M. A. Masterskikh, *Manual on Predicting Frontal Bores* (Gidrometeoizdat, Leningrad, 1980) [in Russian].